IFIC/00-87
FTUV-00-1221
June 22, 2001

Results from Bottomonia Production at the Tevatron and Prospects for the LHC *

J.L. Domenech-Garret[a†] **and M.A. Sanchis-Lozano**[b,c‡]

(a) Departamento de Física Atómica, Molecular y Nuclear
(b) Instituto de Física Corpuscular (IFIC), Centro Mixto Universidad de Valencia-CSIC
(c) Departamento de Física Teórica
Dr. Moliner 50, E-46100 Burjassot, Valencia (Spain)

June 22, 2001

Abstract

We extend our previous analysis on inclusive heavy quarkonia hadroproduction to the whole $\Upsilon(nS)$ (n=1,2,3) resonance family. We use a Monte Carlo framework with the colour-octet mechanism implemented in the PYTHIA event generator. We include in our study higher order QCD effects such as initial-state emission of gluons and Altarelli-Parisi evolution of final-state gluons. We extract some NRQCD colour-octet matrix elements relevant for $\Upsilon(nS)$ (n=1,2,3) hadroproduction from CDF data at the Fermilab Tevatron. Then we extrapolate to LHC energies to predict prompt bottomonia production rates. Finally, we examine the prospect to probe the gluon density in protons from heavy quarkonia inclusive hadroproduction at high transverse momentum and its feasibility in LHC general-purpose experiments.

PACS numbers: 12.38.Aw; 12.39.Jh; 13.85.Ni; 14.40.Gx
Keywords: Quarkonia production; Bottomonium; NRQCD; Tevatron; LHC; gluon density

*Research partially supported by CICYT under grant AEN99-0692
†domenech@evalo1.ific.uv.es
‡Corresponding author: mas@evalo1.ific.uv.es

1 Introduction

Although the main goal of the LHC machine is the search for and the study of the physics beyond the Standard Model, the expected huge rates of bottom quark production make especially interesting the foreseen B physics programme for the LHC project. In fact a specific experiment (LHCb) will focus on B physics, while the two general-purpose experiments ATLAS and CMS will dedicate special periods for data taking to this aim (see for example Ref. [1]). Among heavy flavour physics, heavy quarkonia production and decays have historically played a very important role in the development and test of Quantum Chromodynamics (QCD) as the best candidate to account for the strong interaction dynamics, and likely will continue keeping an outstanding position in this task.

Moreover, over the last decade hadroproduction of heavy quarkonia has received a lot of attention from both theoretical and experimental viewpoints, to explain the discrepancy between the so-called colour-singlet model (CSM) and the experimental data, amounting to a factor of about 50 for direct J/ψ hadroproduction at the Tevatron. In particular, the colour-octet mechanism (COM) [2] can be viewed as the (relativistic) generalization of the CSM and hence the most natural explanation for the unexpected surplus of heavy resonance hadroproduction. Nevertheless, when applied to other production processes like photoproduction at HERA, problems initially arose which cast doubts on the validity of the COM, although recent progress has been done allowing for a better understanding of the situation [3]. Furthermore, results from Tevatron on charmonia polarization (one of the foremost predictions of the COM) seem to indicate even the failure of a naive application of the colour production mechanisms for charmonia [4].

However, the COM can be viewed as deriving from a low energy effective theory, the Non Relativistic QCD (NRQCD) [5], so the question actually arising is whether NRQCD is the correct framework to deal with quarkonia production and decay. Perhaps the v expansion does not converge well for charmonium and subleading contributions cannot be neglected; perhaps the heavy quark spin symmetry is broken to a larger extent than expected. More work in this regard is required to clarify the situation. On the other hand possibly NRQCD is appropriate to describe bottomonia states and their production because of the larger mass of the bottom quark. Hence checking the COM in bottomonia hadroproduction is one of the challenges of strong interaction physics over the next years. Indeed there are alternative models in the literature (based on QCD) trying to explain the experimental facts (see for example [6, 7]). More astringent tests of heavy quarkonia production are thus required to enlight the situation, which can be qualified as rather confusing at present [4].

In a series of previous works ([8, 9, 10, 11, 12, 13]) we have extensively analyzed charmonium hadroproduction in a Monte Carlo framework, using PYTHIA 5.7 [14, 15] event generator with the colour-octet model implemented as a new routine in the generation code [10]. Basically, such a production mechanism is based on the formation of an intermediate coloured state during the hard partonic interaction, evolving non-perturbatively into physical heavy resonances in the final state with certain probabilities governed by NRQCD [5]. In this work we extend our previous study of the $\Upsilon(1S)$ resonance [16, 17] to the whole $\Upsilon(nS)$ family below open bottom production, i.e. $n = 1, 2, 3$, using the CTEQ4L parton distribution function (PDF). A similar analysis can be found in Ref. [18] although limited to transverse momentum (p_T) values higher than 8 GeV.

Although the discrepancies between the CSM and experimental cross sections on bot-

tomonia hadroproduction are smaller than those found for charmonia [19], still some extra contribution should be invoked to account for the surplus observed at the Fermilab Tevatron. However, we find that, analogously to the charmonium case [10], those matrix elements (MEs) determined from Tevatron data in other analyses [20] have to be lowered once initial-state radiation of gluons is taken into account. This is because of the raise of an (*effective*) intrinsic momentum (k_T) of the interacting partons enhancing the moderate and high-p_T tail of the differential cross section for heavy quarkonia production (for more details see Ref. [10]). This effect, as generated by the appropriate PYTHIA algorithm [14, 21], is more pronounced - and likely more sound from a physical viewpoint - than a pure Gaussian smearing with a (required) large $< k_T >$ value. Besides PYTHIA, in smoothing the production cross section, endows us with the possibility of extending our analysis to the small p_T region of bottomonium production, keeping the assumption on the validity of the cross section factorization.

The study of bottomonia production in hadron colliders should permit a stringent test of the colour-octet production mechanism, particularly regarding the predicted (mainly transverse) polarization of the resonance at high-p_T [22], whereas other approaches, like the colour evaporation model, predict no net polarization; indeed, LHC experiments will cover a wider range of transverse momentum than at the Tevatron, allowing to explore the region $p_T^2 >> 4m_b^2$, where m_b denotes the bottom quark mass.

In this paper we also present the prospects to probe the gluon density of protons via heavy quarkonia inclusive hadroproduction at high transverse momentum in the LHC. Our proposal should be viewed along with other related methods of constraining the gluon distribution in hadrons like di-jet, lepton pair and prompt photon production [23, 24, 25]. We must clearly state that it relies on the dominance of a particular production mechanism at high p_T (the COM) predicting a dominant contribution from gluon fragmentation. In spite of this and other assumptions (such as the validity of the factorization of the cross section), our feeling is that LHC collaborations should keep an open mind on all the possibilities offered by the machine, thereby exploring the feasibility of this proposal. For all these and other physical reasons, it is worth to estimate, as a first step, the foreseen production rate of bottomonium resonances at the LHC and this constitutes one of the goals of this work.

We have based our analysis of bottomonia inclusive production on the results from Run IB of the CDF collaboration [19, 26, 27] at the Fermilab Tevatron. This means significantly more statistics than the data sample from Run IA, employed in a former analysis [20]. However, the different sources of prompt $\Upsilon(1S)$ production were not yet separated along the full accessible p_T-range, in contrast to charmonium production. Hence we give in Section 2 the numerical values for some relevant combinations of long-distance MEs, including *direct* and *indirect* $\Upsilon(nS)$ inclusive production, extracted from the fit to the CDF experimental points. (Prompt resonance production includes both direct and indirect channels, the latter referring to feeddown from higher $\Upsilon(nS)$ and $\chi_{bJ}(nP)$ states.) Nevertheless, we still are able to estimate some colour-octet MEs for *direct* $\Upsilon(1S)$ production from the measurements on different production sources at $p_T > 8$ GeV [27]. The extrapolation to LHC is shown in Section 3 where we show the predicted differential and integrated cross section for all $\Upsilon(nS)$ resonances. In Section 4 we discuss heavy quarkonia inclusive hadroproduction as a probe of the gluon density in protons. Finally, in the appendices at the end of the paper, we gather those technical details and values of the parameters employed in the generation.

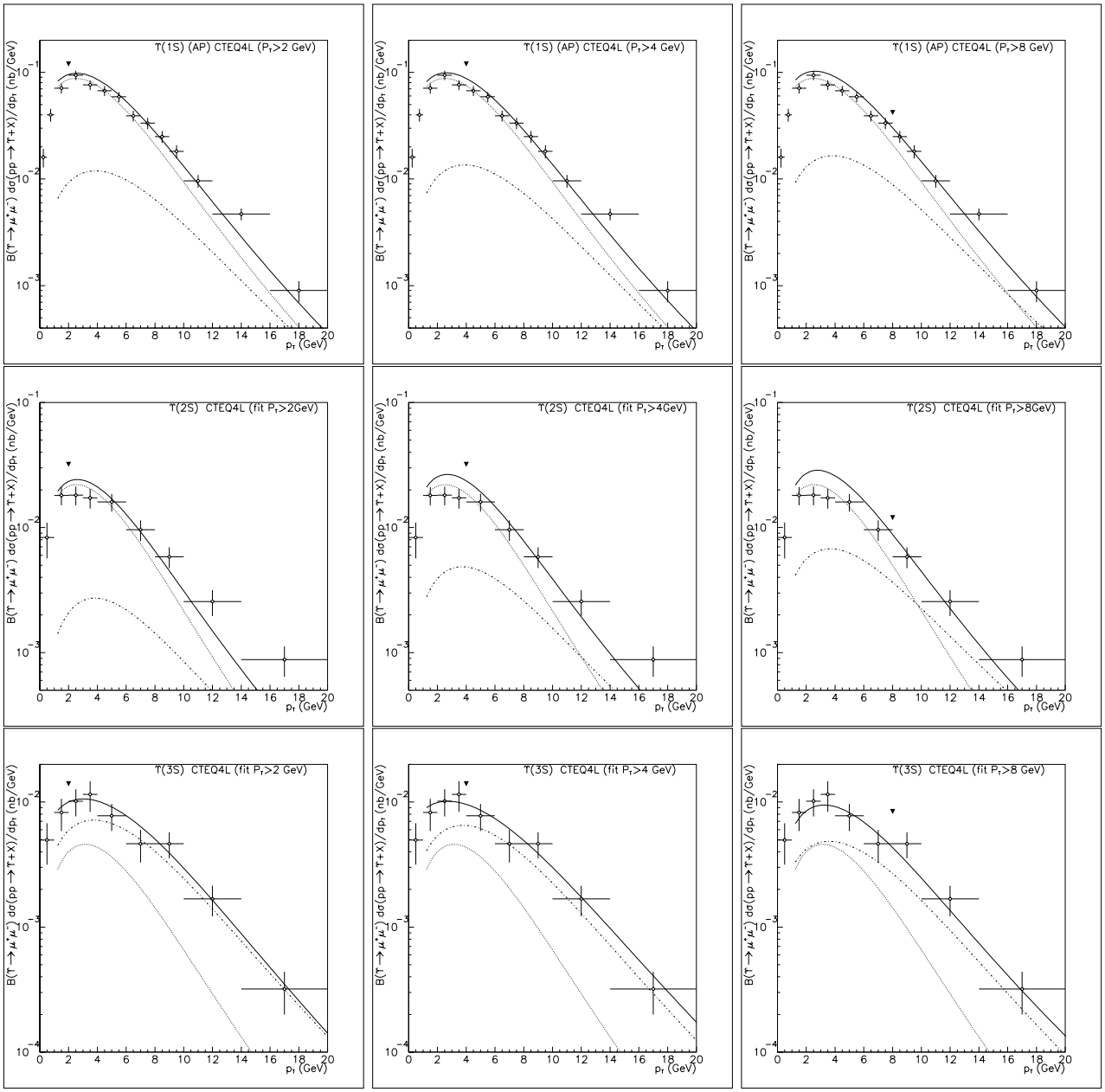

Figure 1: Different fits to the Tevatron data on bottomonia inclusive production in the rapidity interval $|y| < 0.4$ using CTEQ4L PDF and $m_b = 4.88$ GeV. *First row panels*: $\Upsilon(1S)$; *Second row panels*: $\Upsilon(2S)$; *Third row panels*: $\Upsilon(3S)$. Dot, dot-dash and solid lines correspond to the CSM, COM ($^3S_1^{(8)}$ only) and all contributions, respectively. The triangle mark indicates the p_T lower cut-off used in the fit for each case: 2, 4 and 8 GeV. However, we plot the resulting curves extrapolating back over $p_T > 1$ GeV in all cases.

2 Fits to Tevatron data

As briefly outlined in the Introduction, the theoretical differential cross sections on inclusive production of bottomonia would stand above Tevatron experimental points for relatively high p_T if the set of long-distance parameters from [20] were "blindly" employed in the PYTHIA generation running with initial-state radiation on. This is the analogous conclusion which one of us (M.A.S.L.) reached to in the equivalent analysis performed on charmonia hadroproduction [10]. Indeed the smearing caused by multiple emission of gluons by the interacting partons is not limited to small p_T values as could be initially thought, but its influence spreads over a larger region of transverse momenta. In fact we have checked, from a fit to the $\Upsilon(3S)$ differential cross section, that actually this effect amounts to a pretty large value for the effective $< k_T >$ of about 2 GeV, as we shall discuss more extensively in Section 2.2.

Therefore we performed a new analysis of bottomonia CDF data [26], incorporating both direct and indirect production through the CSM (as a "fixed" contribution which, in fact, is dominant at low and even moderate p_T) and the COM, adjusting the long distance parameters for different cut-offs from best $\chi^2_{DF} \equiv \chi^2/N_{DF}$ fits to the experimental points, using the CTEQ4L PDF. If not explicitly stated the contrary, we are turning on initial-state radiation in addition to a Gaussian primordial k_T distribution (with $\sigma = 0.44$ GeV, by default in PYTHIA) in all generations.

2.1 Extraction of the colour-octet MEs

In Figure 1 we show the theoretical curves obtained from our fits to CDF data. In general, nice fits, with χ^2_{DF} values not too far from unity, were found, especially in the $\Upsilon(3S)$ case; instead, the $\Upsilon(2S)$ came out to be the worst one. Let us stress that in the fitting procedure we excluded any possible *negative* contribution from the different channels at the cross section level, in contrast to [18]. Hence we had to dismiss any contribution from the ${}^1S_0 + {}^3P_J$ channels or, in other words, we set the M_5 long-distance parameter (as defined in appendix A) equal to zero, since any positive contribution from this channel would lead to a worse χ^2_{DF} value in all cases.

Table 1: Values of $< O_8^{\Upsilon(nS)}({}^3S_1) > |_{tot}$; $n = 1, 2, 3$ (in units of 10^{-3} GeV^3) from the best fits to CDF data at the Tevatron on prompt $\Upsilon(nS)$ inclusive production for different p_T lower cuts. We also provide the χ^2_{DF} value for each case. The CTEQ4L PDF was used with initial-state and AP evolution activated in PYTHIA.

p_T cut-off:	2 GeV	χ^2_{DF}	4 GeV	χ^2_{DF}	8 GeV	χ^2_{DF}
$1S$	77±17	1.74	87±16	1.53	106±13	1.00
$2S$	40±29	2.87	73±18	1.58	103±27	1.87
$3S$	99±11	1.00	91±15	1.00	68±11	1.00

In Table 1 we show the values of $< O_8^{\Upsilon(nS)}({}^3S_1) > |_{tot}$ ($n = 1, 2, 3$), as defined in (A.7), for different p_T lower cut-offs, in correspondence with the plots of Figure 1. All values are

roughly of order 10^{-1} GeV^3 and agree, within the errors, with the results obtained for $p_T > 8$ GeV by the authors of Ref. [18] using the CTEQ5L parton distribution function.

Nevertheless, let us stress that our numerical estimates for the colour-octet MEs have to be viewed with some caution because of the theoretical and "technical" (due to the Monte Carlo assumptions) uncertainties. For example, our algorithm for AP evolution (see appendix B) should be regarded as a way of reasonably steepening the high-p_T tail of the (leading-order) differential cross section, which otherwise would fall off too slowly as a function of p_T.

2.1.1 Separated production sources for $p_T > 8$ GeV

Current statistics does not permit to subtract indirect production sources to obtain the direct $\Upsilon(1S)$ production cross section along the full accessible p_T-range. Nevertheless, feeddown from higher states ($\Upsilon(nS)$, $\chi_{bJ}(nP)$) was experimentally separated out for $p_T > 8$ GeV [19, 27]. We used this information to check our analysis *a posteriori* (rather than using it as a constraint in the generation) and to draw some important physical conclusions. To this end the relative fractions of the contributing channels for $p_T > 8$ GeV are reproduced in Table 2 from Ref. [19, 27]. On the other hand, we show in Table 3 (which updates our results presented in Ref. [16] using CTEQ2L) the fractions found in this work corresponding to the different generated channels for $p_T > 8$ GeV, following the notation introduced in appendix A.

Table 2: Relative fractions (in %) of the different contributions to $\Upsilon(1S)$ production from CDF data at $p_T > 8$ GeV [27]. Statistical and systematic errors have been summed quadratically.

contribution	Tevatron results
direct $\Upsilon(1S)$	50.9±12.2
$\Upsilon(2S)$+$\Upsilon(3S)$	11.5±9.1
$\chi_b(1P)$	27.1±8.2
$\chi_b(2P)$	10.5±4.6

Table 3: Relative fractions (in %) of the different contributions to $\Upsilon(1S)$ production at the Tevatron for $p_T > 8$ GeV from our generation. Possible contributions from $\chi_{bJ}(3P)$ states were not generated.

contribution	our generation
$\Upsilon(1S)\vert_{^3S_1^{(8)}}$	36.8
$\Upsilon(1S)\vert_{CSM}$	19.5
$\Upsilon(2S)$+$\Upsilon(3S)\vert_{CSM}$	3.9
$\chi_b(1P)\vert_{CSM}$	24.1
$\chi_b(2P)\vert_{CSM}$	15.7

By comparison between Tables 2 and 3 we can conclude that the $\Upsilon(1S)$ indirect production from χ_{bJ}'s decays is almost completely accounted for by the CSM according to the

assumptions and values of the parameters presented in appendix A. Indeed, experimentally 37.6±9.4% of $\Upsilon(1S)$ production is due to $\chi_{bJ}(1P)$ and $\chi_{bJ}(2P)$ decays [27] while from our generation we find a similar global value, namely 39.8%, coming exclusively from colour-singlet production! Moreover, assuming that a 7.6% from the 36.8% fraction (corresponding to the colour-octet $^3S_1^{(8)}$ contribution as expressed in Eq. (A.7)) can be attributed to the $\Upsilon(2S) + \Upsilon(3S)$ channel in addition to the colour-singlet contribution (3.9%), we obviously get the fraction 11.5% for the latter, bringing our theoretical result into agreement with the experimental value. This single assignment implies to reproduce quite well the experimental fraction ($\approx 51\%$) of direct $\Upsilon(1S)$ production by adding the remaining $^3S_1^{(8)}$ contribution to the $\Upsilon(1S)_{CSM}$ channels ($\approx 49\%$) in our generation.

Of course all the above counting was based on mean values from Table 2 and subject to rather large uncertainties. Nevertheless, apart from the consistency of our generation w.r.t. experimental results under minimal assumptions, we can conclude again as in [16] that there is almost *no need for* $\Upsilon(1S)$ indirect production from feeddown of χ_{bJ} states produced through *the colour-octet mechanism*. In other words, the relative contribution from P-wave states to $< O_8^{\Upsilon(1S)}(^3S_1) > |_{tot}$ in Eq. (A.7) should be quite smaller than naïvely expected from NRQCD scaling rules compared to the charmonium sector, in agreement with some remarks made in [28] and recent results found in [18]. The underlying reason for this discrepancy w.r.t. other analyses [20] can be traced back to the dominant colour-singlet contribution to the cross section at p_T values as much large as $\simeq$ 18 GeV (see Figure 1) caused by the effective k_T smearing - already applied to charmonium hadroproduction by one of us [10].

On the other hand the corresponding velocity scaling rule in the bottomonium sector is roughly verified as we shall see. Defining the ratios of matrix elements:

$$R_v(n) \;=\; \frac{< O_8^{\Upsilon(nS)}(^3S_1) > |_{tot}}{< O_1^{\Upsilon(nS)}(^3S_1) > |_{tot}} \;, \tag{1}$$

its values, shown in Table 4, are in accordance with the expected order-of-magnitude $v^4 \approx 0.01$, where v is the relative velocity of the bottom quark inside bottomonium. Nevertheless we realize an increase of $R_v(n)$ for higher n values. Assuming that the $< O_8^{\Upsilon(nS)}(^3S_1) > |_{tot}$ matrix element could be interpreted as a (weighted) colour-octet wave function squared (in the same way as $< O_1^{\Upsilon(nS)}(^3S_1) > |_{tot}$ w.r.t. the colour-singlet state, see appendix A) the ratio $R_v(n)$ of both squared wave functions in the origin comes out as not independent of the resonance state under consideration.

Table 4: Values (in units of GeV^3) of different colour-singlet and colour-octet combinations of MEs according to Eqs. (A.4) and (A.7) and the ratios $R_v(n)$; $n = 1, 2, 3$. The best χ^2_{DF} values from Table 1 are displayed.

Resonance	$< O_1^{\Upsilon(nS)}(^3S_1) > \|_{tot}$	$< O_8^{\Upsilon(nS)}(^3S_1) > \|_{tot}$	$R_v(n)$
$\Upsilon(1S)$	11.1	0.106	0.0095
$\Upsilon(2S)$	5.01	0.073	0.0145
$\Upsilon(3S)$	3.54	0.099	0.028

Thus we conclude that this particular NRQCD velocity scaling rule, although valid as an order-of-magnitude estimate, retains a weak dependence on the principal quantum number n, not completely cancelling in the ratio (1).

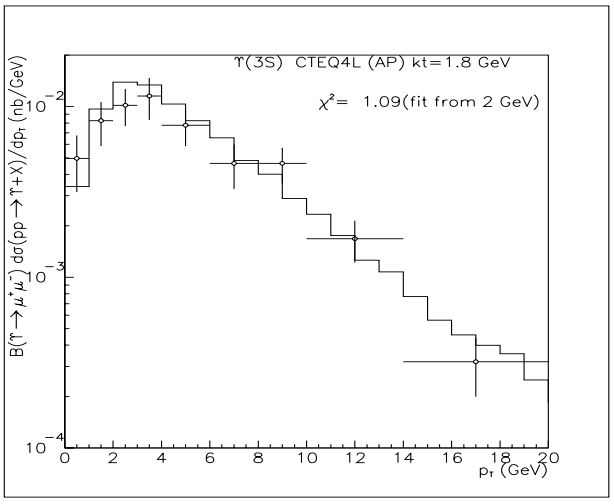

Figure 2: Fit to the Tevatron data on $\Upsilon(3S)$ hadroproduction using a gaussian smearing function with $\sigma = 2$ GeV, i.e. $< k_T >= 1.8$ GeV.

2.2 Gaussian $< k_T >$ smearing

The smearing effect on the differential cross section caused by initial-state radiation of gluons can be roughly simulated by means of a gaussian intrinsic k_T distribution of the interacting partons inside hadrons, to be convoluted with the corresponding hard interaction cross sections:

$$D(\mathbf{k_T}) \;=\; \frac{1}{\pi\sigma^2}\exp\left(-\frac{k_T^2}{\sigma^2}\right) \tag{2}$$

with

$$< k_T > = \;\frac{\sqrt{\pi}}{2}\;\sigma \tag{3}$$

The width of the gaussian can be viewed as an adjustable parameter [29]. In fact PYTHIA incorporates as an option a gaussian primordial k_T smearing, whose width can be set by the user. We used this possibility to make a "new" fit of Tevatron data for the $\Upsilon(3S)$ resonance, employing the same matrix elements as shown in Table 1 but with initial-state radiation off. Then the gaussian k_T smearing has to simulate the (this time missing) initial-state radiation. In Figure 2 we show the resulting histogram, corresponding to a value $\sigma = 2$ GeV, i.e. $< k_T >= 1.8$ GeV.

3 $\Upsilon(nS)$ Production at the LHC

We already mentioned in the Introduction that bottomonium hadroproduction is especially interesting to check the validity of the colour-octet model as often emphasized in the literature [30, 31]. This becomes particularly clear at the LHC since experimental data will spread

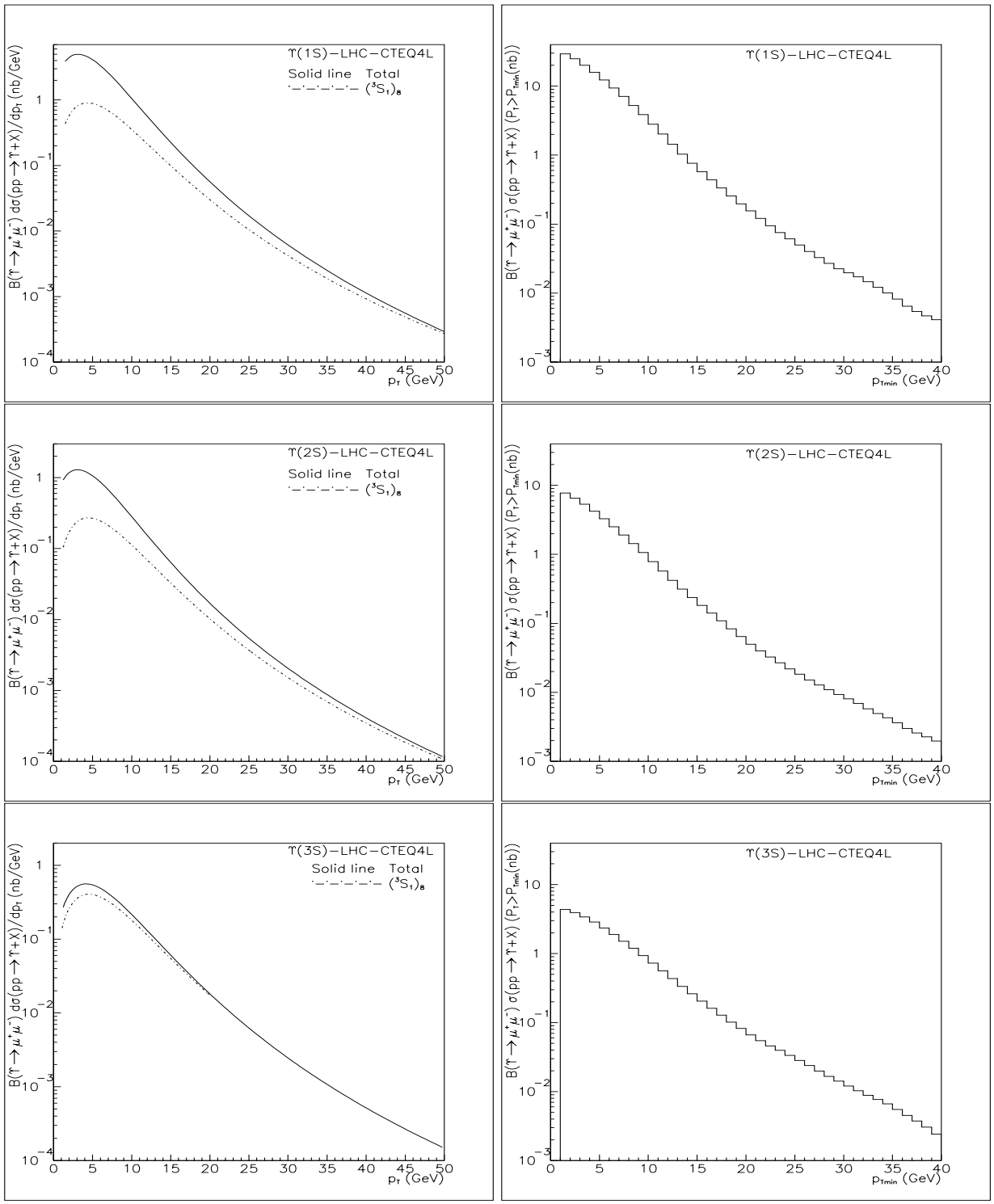

Figure 3: *First row panels, left side* : Predicted prompt $\Upsilon(1S)$ differential cross section (multiplied by the muonic branching fraction) at the LHC using the CTEQ4L PDF and $m_b = 4.88$ GeV. A rapidity cut $|y| < 2.5$ was required for bottomonium. Dot-dashed line: $^3S_1^{(8)}$ contribution; solid line: all contributions. *Right side :* Integrated cross section. *Second and third row panels*: The same as in first row for $\Upsilon(2S)$ and $\Upsilon(3S)$ respectively.

over a wider p_T-range than at the Tevatron, allowing an overall study from low to very high p_T values. Therefore the expected transition of the different production mechanisms along the p_T region could be scrutinized in detail: from gluon gluon fusion at low p_T to the foreseen asymptotically dominant gluon fragmentation into bottomonium states.

Keeping this interest in mind, we used our code implemented in PYTHIA to generate prompt $\Upsilon(nS)$ resonances in proton-proton collisions at a center-of-mass energy of 14 TeV employing the best χ^2_{DF} colour-octet MEs shown in Table 1. In figure 3 the theoretical curves for the $\Upsilon(nS)$ $(n = 1, 2, 3)$ differential and integrated cross sections are exhibited as a function of p_T, including both direct production and feeddown from higher resonance states (except for the $\Upsilon(3S)$).

In Figures 4 we show our prediction for *direct* $\Upsilon(nS)$ production. This is especially interesting if LHC detectors would be able to discriminate among those different sources of resonance production. (See the end of Section 4 and footnote #2.)

To this end we generated $\Upsilon(1S)$ events through both the CSM and COM making use of the following parameters

- $< O_1^{\Upsilon(1S)}(^3S_1) > |_{direct} = 9.28$ GeV^3 (from [28])
- $< O_8^{\Upsilon(1S)}(^3S_1) > |_{direct} = 0.084$ GeV^3

The first value corresponds to the CSM matrix element for direct production while the $< O_8^{\Upsilon(1S)}(^3S_1) > |_{dir}$ value was obtained after removing the $\Upsilon(2S) + \Upsilon(3S)$ contribution according to the discussion made in Section 2.1.1, i.e. under the assumption that a fraction 7.6% from the 36.8% in table 3 should be assigned to indirect production. Finally let us mention that we neglected any contribution from the ${}^1S_0^{(8)} + {}^3P_J^{(8)}$ channels, in accordance with our analysis on Tevatron results of Section 2.

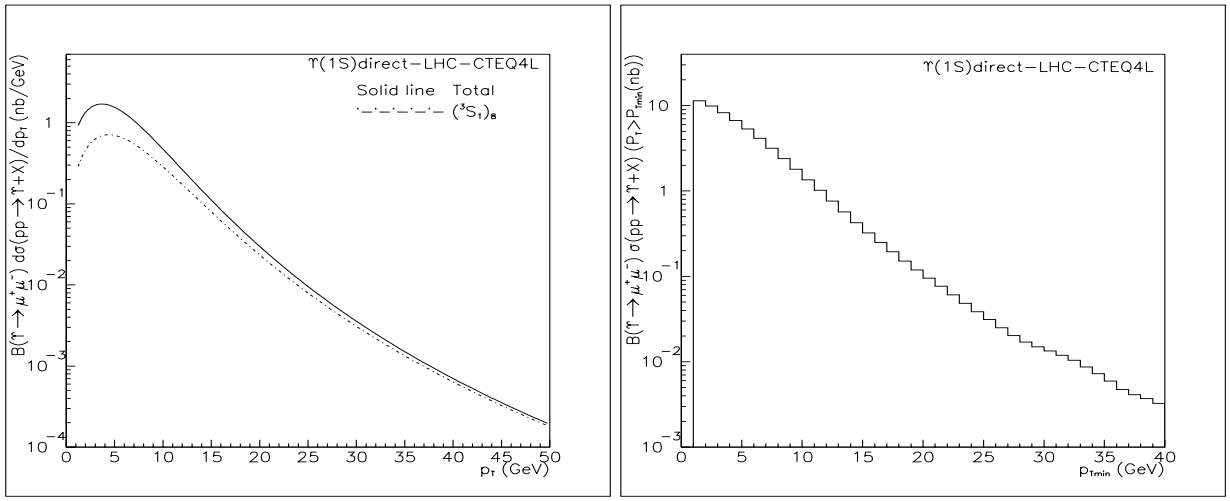

Figure 4: The same as in Figure 3 for *direct* $\Upsilon(1S)$ production at the LHC.

4 Heavy quarkonia inclusive production as a probe of the gluon density in protons

One of the goals of the LHC project is to perform precise tests of the Standard Model of strong, weak and electromagnetic interactions and the fundamental constituents of matter. In fact the LHC machine can be viewed as a gluon-gluon collider to some extent. On the other hand, many signatures (and their backgrounds) of physics, both within and beyond the Standard Model, involve gluons in the initial state [1]. Therefore an accurate knowledge of the gluon density in protons acquires a special relevance for all these reasons.

So far, the most precise determinations of the gluon momentum distributions in the proton come from the analysis of the scaling violations of the structure function F_2. However, this represents an indirect method since it is the sea distribution which is actually measured and the gluon density is obtained by means of the QCD evolution equations. On the other hand, hadron-hadron scattering processes with direct photon production or jets in the final state will probably be extremely adequate to probe "directly" the gluon distribution in hadrons. In this Section, we shall examine the possibility of using heavy quarkonia inclusive production in proton-proton collisions at the LHC, in a complementary way to those studies. However, there are still many uncertainties and pending questions regarding quarkonia hadroproduction despite the existence of NRQCD [5], an effective theory coming from first principles, which should provide an adequate framework for this kind of processes involving both perturbative and non-perturbative aspects of the strong interaction dynamics. Likely, forthcoming experimental data - and their respective analyses - from Tevatron and other machines like HERA, should clarify the situation before LHC becomes operative.

In the following we shall focus on very high p_T production of bottomonia states. Therefore the main production mechanism according to the COM should be through the partonic subprocess:

$$g\ g \rightarrow g^*\ g \tag{4}$$

followed by the gluon fragmentation into a $\Upsilon(nS)$ state:

$$g^* \rightarrow \Upsilon(nS)\ X \quad ;\ (n = 1, 2, 3) \tag{5}$$

produced through a colour-octet mechanism. On the other hand, the bottom mass is large enough to justify the colour-octet model applied to quarkonium hadroproduction. Whether a similar approach could be applied to charmonium resonances has to be checked, for example analyzing the transverse polarization of the resonance.

Ideally, the final state gluon (g) in Eq. (4) will give rise to a recoiling jet ($g \rightarrow jet$), sharing, in principle, the same transverse momentum as the heavy resonance (in absence of higher order corrections; see however appendix C). Hence events would topologically consist of an almost isolated muon pair from the decay of the heavy resonance and a recoiling jet. Indeed one should expect a $\mu^+\mu^-$ pair almost isolated because the energy difference between the masses of the intermediate coloured and final states is assumed to be rather small (of the order of $m_b v^2 \simeq 500$ MeV) then allowing the emission of eventually a few light hadrons via soft gluon radiation at the final hadronization stage.

Bottomonia production coming from fragmenting gluons in QCD jets (an alternative production mechanism, see [32]) should not exactly display the same signature as the hard α_s^3 processes. Indeed, the muon pair would be embedded in one of the two jets - not so much

isolated as in the process (4-5) due to the production cascade - and its momentum should not balance the momentum of the other event jet to the same extent. In sum, the signature of an almost isolated muon pair recoiling against a jet with an approximate momentum balance in the transverse plane, should provide a suitable tag for the production mechanism represented in Eqs. (4-5).

We shall assume a tight kinematic cut in this our first approach: Both the rapidity of the heavy resonance and the rapidity associated to the recoiling jet should be around zero. However, in order to increase the foreseen statistics, one could dispense with this constraint by only requiring (within the experimental and theoretical uncertainties) back-to-back production. We shall come back to this issue at the end of this Section.

Developing the idea

In the absence of any intrinsic k_T effect, we can write the triple differential cross section for the inclusive production process $pp \to \Upsilon X$ as

$$\frac{d^3\sigma}{dy_\Upsilon dy_{jet} dp_T} = 2p_T \sum_{ab} x_a x_b f_{a/p}(x_a) f_{b/p}(x_b) \frac{d\hat{\sigma}_{ab}}{d\hat{t}} \tag{6}$$

where $f_{a/p}(x_a)$ denotes the parton-a density in the proton, and

$$\frac{d\hat{\sigma}_{ab}}{d\hat{t}} \equiv \frac{d\hat{\sigma}}{d\hat{t}}(ab \to \Upsilon c) = \frac{1}{16\pi \hat{s}^2} \overline{\sum} |\mathcal{A}(ab \to \Upsilon c)|^2 \tag{7}$$

stands for the partonic differential cross section (the barred summation denotes an average over initial and final spins and colours) consisting of a short distance (and calculable) part and a long distance part which can be identified as a colour-octet matrix element according to NRQCD. This factorization of the cross section was established on solid grounds in Ref. [5] within the NRQCD framework.

As above-mentioned we shall require both rapidities (of the Υ and the recoiling jet) to be less than a common small value y_0: $|y_\Upsilon| < y_0$, $|y_{jet}| < y_0$. We could set $y_0 = 0.25$ for example, as discussed in appendix C.) Then $x_a \simeq x_b = x$, and

$$x_a x_b = x^2 = \frac{\hat{s}}{s} \tag{8}$$

At very high p_T (i.e. $p_T^2 >> 4m_b^2$) we can identify $\hat{s} \approx 4p_T^2$. (Hereafter we consider $p_T \geq 20$ GeV.) Therefore measuring the transverse momentum of the resonance should lead to the the knowledge of the momentum fraction x of the interacting partons, with a typical uncertainty (see appendix C)

$$\frac{\Delta x}{x} \;=\; y_0 \tag{9}$$

In particular the dominant partonic subprocess should be the gluon-gluon interaction. Thus the gluon density $G(x, \mu^2)$ in the proton will mainly be involved and we can write as a first approximation

$$\frac{d^3\sigma}{dy_\Upsilon dy_{jet} dp_T} = 2p_T \; x^2 \; G(x, \mu^2)^2 \; \frac{d\hat{\sigma}_{gg}}{d\hat{t}} \tag{10}$$

where we can choose, for example $\mu^2 \;=\; \hat{s}$

The proposal [1]

We propose to study the ratios:

$$\frac{x_2^2\ G(x_2,\mu_2^2)^2}{x_1^2\ G(x_1,\mu_1^2)^2}\ =\ \left(\frac{d\hat{\sigma}_{gg}/d\hat{t}_1}{d\hat{\sigma}_{gg}/d\hat{t}_2}\right)\times\left(\frac{p_{T1}}{p_{T2}}\right)\times\left(\frac{d^3\sigma/dy_\Upsilon dy_{jet}dp_{T2}}{d^3\sigma/dy_\Upsilon dy_{jet}dp_{T1}}\right) \tag{11}$$

for a set of x_1, x_2 pairs and *different gluon distributions*. The number of pairs is basically limited by Δx, i.e. y_0, so this constraint cannot released too much (see appendix C).

Therefore the keypoint is to consider the l.h.s. of the above equality (Eq. (11)) as an *input* corresponding to different sets of the gluon distribution for the proton, whose x dependence is hence assumed to be "known", and in fact would be tested. On the other hand the r.h.s. corresponds to an input from experimental data and some theoretical factors likely under control.

Let us remark that the x and μ^2 values are *not independent* in this proposal; indeed for each value of x, μ^2 is fixed by $\hat{s} = x^2 s$. However, notice that the scale can actually be varied by choosing a different assignment for μ^2, e.g. $\mu^2 = \hat{s}/4$.

Next we shall write expression (11) as

$$\frac{x_2^2\ G(x_2,\mu_2^2)^2}{x_1^2\ G(x_1,\mu_1^2)^2}\ =\ R_{theo}\times R_{exp} \tag{12}$$

where

$$R_{theo}(p_{t1},p_{t2},\mu_1^2,\mu_2^2)\ =\ f_{cor}\times\frac{d\hat{\sigma}_{gg}/d\hat{t}_1}{d\hat{\sigma}_{gg}/d\hat{t}_2} \tag{13}$$

and in the high p_T limit,

$$R_{theo}\to f_{cor}\times\frac{\alpha_s^3(\mu_1^2)\ p_{T2}^4}{\alpha_s^3(\mu_2^2)\ p_{T1}^4}$$

explicitly showing that $\alpha_s(\mu^2)$ is entangled in the gluon density determination. On the other hand, note that the dependence on the NRQCD matrix elements does cancel in R_{theo}, but there is a dependence on the scales μ_1^2 and μ_2^2, which should match the same dependence in the left hand side. We have incorporated some possible corrections through the f_{cor} factor - which could be calculated either analytically or by Monte Carlo methods - taking into account higher-order effects such as intrinsic k_T of the interacting gluons, AP evolution of the fragmenting gluons, etc.

On the other hand the experimental input reads as the ratio

$$R_{exp}(p_{T1},p_{T2},y_0)=\left(\frac{p_{T1}}{p_{T2}}\right)\times\left(\frac{d^3\sigma/dy_\Upsilon dy_{jet}dp_{T2}}{d^3\sigma/dy_\Upsilon dy_{jet}dp_{T1}}\right) \tag{14}$$

which can be obtained directly from experimental data.

[1] Presented at the UK Phenomenology Workshop on Heavy Flavour and CP violation, Durham, September 2000 [33] and at the B physics working group meeting of the ATLAS collaboration held at CERN in October, 2000 [34].

Introducing the gluon quark contribution

Although expectedly dominant, the gluon gluon partonic subprocess is not the only α_s^3 contribution to the cross section yielding a fragmenting gluon into $\Upsilon(nS)$ at high p_T. Also gluon quark scattering $gq \to g^* q$ followed by $g^* \to \Upsilon(nS)X$, can give a sizeable contribution (about 20% at $p_T > 20$ GeV, see table 6 in appendix A). Consequently, the expression (12) for the ratio of gluon densities has to be modified to include the quark distribution $q(x, \mu^2)$ in protons:

$$\frac{x_2 G(x_2, \mu_2^2)\ (x_2 G(x_2, \mu_2^2) + k{\cdot}x_2 q(x_2, \mu_2^2))}{x_1 G(x_1, \mu_1^2)\ (x_1 G(x_1, \mu_1^2) + k{\cdot}x_1 q(x_1, \mu_1^2))} \ = \ R_{theo} \times R_{exp} \tag{15}$$

where k is a factor taking into account the ratio of the gq and gg cross sections, both calculated at the same values of the Mandelstam variables $\hat{s}$ and $\hat{t}$ of the hard interaction, i.e.

$$k \ = \ \frac{d\hat{\sigma}_{gq}/d\hat{t}}{d\hat{\sigma}_{gg}/d\hat{t}} \tag{16}$$

becoming independent of x (and μ^2) at zero rapidity and large p_T; then $k \simeq 0.2$.

Alternatively, one can write the density ratio as

$$\frac{x_2^2\ G(x_2, \mu_2^2)^2 (1 + k{\cdot}\lambda(x_2, \mu_2^2))}{x_1^2\ G(x_1, \mu_1^2)^2 (1 + k{\cdot}\lambda(x_1, \mu_1^2))} \tag{17}$$

where

$$\lambda(x, \mu^2) = \frac{q(x, \mu^2)}{G(x, \mu^2)}$$

By Taylor expanding the above ratio, the leading term is

$$\frac{x_2^2\ G(x_2, \mu_2^2)^2}{x_1^2\ G(x_1, \mu_1^2)^2}\ (1 + r)$$

where

$$r = k{\times}\Big[\lambda(x_2, \mu_2^2) - \lambda(x_1, \mu_1^2)\Big]$$

should be a quite small quantity. (We have checked with CTEQ4L that typically $r \approx 0.03$ for values between $x_1 = 3{\cdot}10^{-3}$ and $x_2 = 1.5{\cdot}10^{-2}$.)

We can rewrite Eq. (12) as

$$\frac{x_2^2\ G(x_2, \mu_2^2)^2}{x_1^2\ G(x_1, \mu_1^2)^2}(1 + r) = R_{theo} \times R_{exp} \tag{18}$$

Again the l.h.s. is an input from the PDF to be tested, while the r.h.s. comes from experimental data and some theoretical calculations without requiring the NRQCD MEs values.

From an experimental point of view it may happen that the discrimination among the different $\Upsilon(nS)$ states via mass reconstruction could become a difficult task, especially at

very high p_T, because of the uncertainty on the measurement of the muons momenta [1] [2]. Nevertheless, since we are proposing to study *ratios* of cross sections, we can consider the overall $\Upsilon(nS)$ inclusive production, without separating the different bottomonia sources - all the weighted matrix element cancelling in the quotient if we neglect the mass differences between the different states. (Notice that at high p_T there is almost no contribution from the CSM.) In Figure 5 we show the combined production rate at $p_T > 20$ GeV and $|y| < 0.25$ for the upper and lower values of the colour-octet matrix elements shown in Table 1.

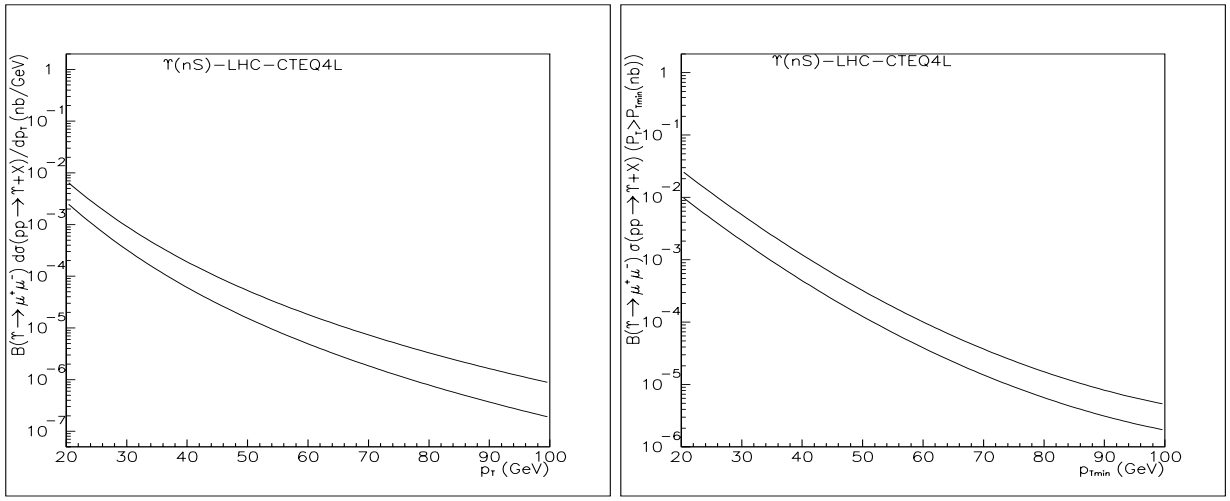

Figure 5: Predicted $\Upsilon(1S)+\Upsilon(2S)+\Upsilon(3S)$ weighted contributions to bottomonia inclusive production at the LHC corresponding to the upper and lower MEs from Table 1, in the rapidity interval $|y| < 0.25$ and $p_T > 20$ GeV. *Left panel*: differential cross section; *right panel*: integrated cross section.

Assuming an integrated luminosity of 10 fb^{-1}, corresponding to one year running (10^7s) of LHC at "low" luminosity (10^{33} cm^{-2}s^{-1}) we can easily get the expected number of events from figures 5, just by multiplying the ordinate by a factor 10^7. Thus we can see that the foreseen number of events (aside efficiency reduction) at $p_T > 20$ GeV is about 10^5, whereas at $p_T > 40$ GeV is about 10^4. By extrapolation we get a meagre expected number of $\simeq 10^2$ events at $p_T > 100$ GeV. This makes unlikely any measurement for transverse momentum larger than 100 GeV, under the tight rapidity cut of 0.25 on the resonance which we are imposing.

In view of the foreseen rates of bottomonia production at the LHC we propose testing the shape of the gluon density in protons for x values ranging in the interval: 3×10^{-3} *to* 1.5×10^{-2}, using $x = \sqrt{\hat{s}/s}$ from $p_T = 20$ GeV up to $p_T = 100$ GeV, under the rapidity constraint $y < 0.25$.

Nevertheless, by removing the condition $|y| < 0.25$ statistics could considerably be enlarged. Since our proposal essentially relies on the determination of the Feynman x of the interacting partons by measuring the p_T of the final products of the reaction, there is still the possibility of requiring a back-to-back topology but sweeping the whole accessible rapidity region $|y| < 2.5$, instead of limiting ourselves to the central rapidity values. This goal can be achieved by selecting events with the muon pair and the recoiling jet sharing common

[2] We thank M. Smizanska for bringing this point to our attention.

values of p_T and absolute rapidities, within the uncertainties. In other words, events could be accepted with both $\Upsilon(nS)$ and recoiling jet rapidities satisfying $||y_\Upsilon| - |y_{jet}|| < 0.25$; in such a way statistics should increase by a factor $\simeq 10$, possibly extending the allowed region of p_T up to higher values than 100 GeV, and hence reaching larger values of the momentum fraction x.

As a final remark, if the colour-octet model is confirmed and the corresponding MEs accurately and consistently extracted from other experiments like Tevatron or HERA - or theoretically computed - one can consider then the possibility of unfolding the gluon density from the measured cross section as proposed, for instance, in Ref. [35] by means of D^* meson production at HERA. In such a case, our proposal would extend beyond the study of ratios, allowing the extraction of gluon and quark densities directly from heavy quarkonia production mechanisms.

5 Summary

In this paper we have analyzed CDF measurements on $\Upsilon(nS)$ $(n = 1, 2, 3)$ inclusive hadroproduction cross sections at the Tevatron in a Monte Carlo framework, extracting some relevant colour-octet NRQCD matrix elements. Higher-order QCD effects such as initial-state radiation and AP evolution of gluons were included in our analysis. The fact that we were able to take into account the effects of soft-gluon emission in the initial-state (according to the PYTHIA machinery) yielding a smooth p_T behaviour at low p_T, allowed us to extend the study of the differential cross section down to $p_T = 2$ GeV. However, in order to study the sensitivity to different cut-offs, fits were performed using experimental points above several p_T cut-offs (see Table 1).

On the other hand, since the different sources of $\Upsilon(nS)$ production were not experimentally separated along the full accessible p_T-range we have included all of them in the generation and later fits. Only for $p_T > 8$ GeV, feeddown from χ_{bJ} states was experimentally separated out from direct $\Upsilon(1S)$ production. We used these results as a consistency check of our analysis and to draw some conclusions summarized below.

The numerical value of the $< O_8^{\Upsilon(1S)}(^3S_1) >|_{tot}$ matrix element should be ascribed almost totally to $\Upsilon(nS)$ states. This finding may be surprising when confronted with other analyses [20, 28], where the contribution to the $\Upsilon(1S)$ yield through the colour-octet χ_{bJ} channels was thought as dominant [28, 31, 36]. On the contrary, we concluded from Tables 2 and 3 that the *colour-singlet production* can account by itself for the feeddown of $\Upsilon(1S)$ from χ_{bJ} states. (Notice however that experimental uncertainties still leave some room for a possible COM contribution but to a much lesser extent than previously foreseen [20, 28].) On the other hand the different production channels are consistent (or can be made consistent) with the experimental relative fractions shown in Table 2, after some reasonable assumptions.

We have extended our study to LHC collider experiments ($\sqrt{s} = 14$ TeV center-of-mass energy). In Figure 3 we presented our predictions for prompt production rates (i.e. including direct and indirect production) while in Figure 4 we showed our prediction for direct $\Upsilon(1S)$ production alone.

We conclude that the foreseen yield of $\Upsilon(nS)$'s at LHC energy will be large enough, even at high-p_T, to perform a detailed analysis of the colour-octet production mechanism and should be included in the B-physics programme of the LHC experiments, probably

deserving (together with charmonia) a dedicated data-taking trigger.

On the other hand, we have presented in some detail (but without considering detector effects) the prospects to use heavy quarkonia inclusive production at the LHC (or perhaps at the Tevatron too, using data from the high luminosity Run II) to probe the gluon density in protons. Let us remark that we are renouncing to use any absolute normalization because this would imply a precise knowledge of the colour-octet NRQCD matrix elements governing the transition of the fragmenting gluon into a particular heavy quarkonium state, hence introducing an important uncertainty since they are not accurately known so far. If those NRQCD elements were finally accurately and consistently determined (either theoretically or experimentally) one could then consider the possibility of unfolding the parton densities from LHC experimental data on heavy resonance inclusive production, as described in our proposal. Thus we conclude that: *a)* Inclusive hadroproduction of heavy resonances at high p_T in general-purpose LHC experiments could be a complementary method of constraining the gluon density in protons, along with other related methods: di-jet, lepton pair and prompt photon production; *b)* An experimental advantage of this method lies in the fact that the "flight direction" of a high-p_T fragmenting gluon into a $\Upsilon(nS)$ resonance can be inferred from the muonic pair coming from its decay, thereby providing a clean constraint in the search for the associated recoiling jet, in addition to the self-triggering signature of events.

We finally want to stress the importance of keeping an open mind on the different possibilities offered by the LHC, likely deserving a previous work to prepare in advance jointly experimental strategies and theoretical calculations.

Acknowledgements

We acknowledge interesting discussions with N. Ellis, S. Frixione, M. Krämer, F. Maltoni, M. Smizanska, Y. Tsipolitis and S. Wolf.

References

[1] ATLAS detector and physics performance Technical Design Report, CERN/LHCC/99-15.

[2] E. Braaten and S. Fleming, Phys. Rev. Lett. **74** (1995) 3327.

[3] S. Wolf, hep-ph/0010217.

[4] M. Krämer, hep-ph/0010137.

[5] G.T. Bodwin, E. Braaten, G.P. Lepage, Phys. Rev. **D51** (1995) 1125.

[6] S. Baranov, Phys. Lett. **B388** (1996) 366.

[7] Ph. Hägler *et al.*, hep-ph/0004263.

[8] M.A. Sanchis-Lozano and B. Cano, Nucl. Phys. B (Proc. Suppl.) 55A (1997) 277 (hep-ph/9611264).

[9] B. Cano-Coloma and M.A. Sanchis-Lozano, Phys. Lett. **B406** (1997) 232.

[10] B. Cano-Coloma and M.A. Sanchis-Lozano, Nucl. Phys. **B508** (1997) 753.

[11] M.A. Sanchis-Lozano, Nucl. Phys. B (Proc. Suppl.) 75B (1999) 191 (hep-ph/9810547).

[12] M.A. Sanchis-Lozano, Nucl. Phys. B (Proc. Suppl.) 86 (2000) 543 (hep-ph/99707497).

[13] P. Nason *et al*, hep-ph/0003142.

[14] T. Sjöstrand, Comp. Phys. Comm. **82** (1994) 74.

[15] T. Sjöstrand *et al.*, hep-ph/0010017.

[16] J.L. Domenech and M.A. Sanchis-Lozano, Phys. Lett. **B476** (2000) 65.

[17] J.L. Domenech and M.A. Sanchis-Lozano, hep-ph/0010112.

[18] E. Braaten, S. Fleming and A. Leibovich, hep-ph/0008091.

[19] CDF Collaboration, Phys. Rev. Lett. **69** (1992) 3704.

[20] P. Cho and A.K. Leibovich, Phys. Rev. **D53** (1996) 6203.

[21] T. Sjöstrand, Phys. Lett. **B157** (1985) 321.

[22] E. Braaten and J. Lee, hep-ph/0012244.

[23] H.L. Lai *et al.*, CTEQ Collaboration, Eur. Phys. J. **C12** (2000), hep-ph/9903282.

[24] E.L. Berger and M. Klasen, hep-ph/0003211.

[25] A.D. Martin *et al.*, hep-ph/9907231.

[26] G. Feild *et al.*, CDF note 5027.

[27] CDF Collaboration, CDF note 4392.

[28] G. Schuler, Int. J. Mod. Phys. **A12** (1997) 3951.

[29] K. Sridhar, A.D. Martin, W.J. Stirling, Phys. Lett. **B438** (1998) 211.

[30] M. Beneke and M. Krämer, Phys. Rev. **D55** (1997) 5269.

[31] A. Tkabladze, Phys. Lett. **B462** (1999) 319.

[32] S. Baranov, to appear in Nucl. Phys. B (Proc. Suppl.) of the IV Int. Conf. on Hyperons, charm and beauty hadrons, Valencia, June 2000.

[33] S. Frixione *et al.*, to appear in the Proceedings of the UK Phenomenology Workshop on Heavy Flavour and CP Violation, Durham, 17-22 September 2000.

[34] Transparencies available under request to the authors.

[35] H1 Collaboration, Nucl. Phys. **B545** (1999) 21.

[36] M. Beneke, CERN-TH/97-55, hep-ph/9703429.

[37] D.E. Groom *et al.*, Particle Data Group, EPJ **C15** (2000) 1.

[38] E.J. Eichten and C. Quigg, Phys. Rev. **D52** (1995) 1726.

Appendices

A

Some technical details for the generation with PYTHIA

Basically we reproduce here the information given in [16] about the values of the parameters and options set in running PYTHIA, with some more details.

Originally the event generator PYTHIA 5.7 produces direct J/ψ and higher χ_{cJ} resonances via the CSM only [14]. It is not a difficult task to extend this generation to the bottomonium family by redefining the resonance mass and wave function parameter accordingly. In our analysis we have besides implemented a code in the event generator to account for the colour-octet production mechanism via the following α_s^3 partonic processes:

$$g \ + \ g \rightarrow (Q\overline{Q})[^{2S+1}X_J] \ + \ g \tag{A.1}$$

$$g \ + \ q \rightarrow (Q\overline{Q})[^{2S+1}X_J] \ + \ q \tag{A.2}$$

$$q \ + \ \overline{q} \rightarrow (Q\overline{Q})[^{2S+1}X_J] \ + \ g \tag{A.3}$$

where $(Q\overline{Q})[^{2S+1}X_J]$ stands for a certain heavy quarkonium state denoted by its spectroscopic notation (see Refs. [20, 10] for more details). In particular we have considered the $^3S_1^{(8)}$, $^1S_0^{(8)}$ and $^3P_J^{(8)}$ contributions as leading-order intermediate coloured states. In addition we generated $\Upsilon(nS)$ $(n = 1, 2, 3)$ and $\chi_{bJ}(nP)$ $(n = 1, 2)$ resonances decaying into $\Upsilon(1S)$, according to the CSM as mentioned above.

Table 5: $^3S_1^{(8)}$ contributions to the $\Upsilon(1S)$ cross section at the Tevatron for $p_T > 8$ GeV

Contribution	%
gg	69
qg	30
$q\overline{q}$	1

Table 6: $^3S_1^{(8)}$ contributions to the $\Upsilon(1S)$ cross section at the LHC for $p_T > 8$ GeV

Contribution	%
gg	80
qg	20
$q\overline{q}$	$\simeq 0$

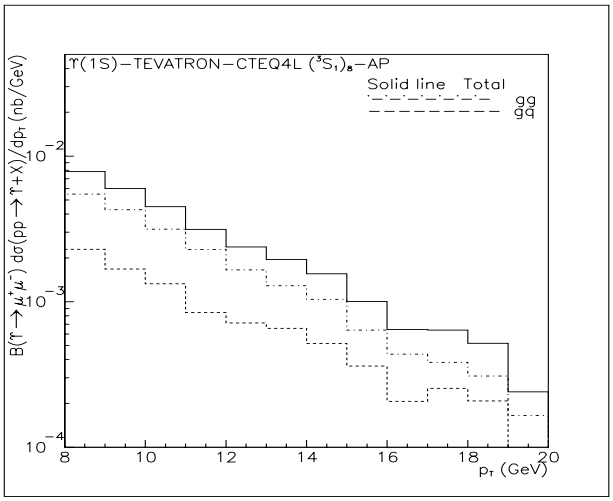

Figure 6: Gluon-gluon versus quark-gluon ${}^3S_1^{(8)}$ contributions from our $\Upsilon(1S)$ generation at the Tevatron for $p_T > 8$ GeV. The latter becomes more and more important at larger p_T as could be expected since higher Feynman x of partons in the proton are involved and the gq contribution becomes increasingly more significant w.r.t. the gg one.

A p_T lower cut-off was set equal to 1 GeV (by default in PYTHIA) throughout the generation since some of the contributing channels are singular at vanishing transverse momentum [12]. Furthermore, all fits of Tevatron data were performed using p_T values above 2 GeV.

We find from our simulation (see Tables 5 and 6) that gluon-gluon scattering actually stands for the dominant process at high p_T as expected, gluon-quark scattering contributes appreciably however ($\simeq 20-30\%$ of the colour-octet production cross section) whereas the quark-antiquark scattering represents a quite small fraction ($\simeq 1\%$ at the Tevatron). In Figure 6 we plot the gluon-gluon and quark-gluon ${}^3S_1^{(8)}$ contributions as a function of the transverse momentum of the resonance obtained from our generation for the Tevatron. This kind of information could be particularly interesting for our discussion on the probe of the gluon density in protons developed in Section 4.

Set of "fixed" and free parameters used in the generation

Below we list the main parameters, including masses and branching fractions, used in our generation with PYTHIA 5.7. We employed the CTEQ4L parton distribution function (PDF) in all our analysis.

Masses and branching fractions:

- $m_b = 4.88$ GeV
- $m_{resonance} = 2m_b$ in the theoretical calculation of the cross sections for the short-distance processes [20]. In the phase space factors for the event

generation we set, however, real masses of the $\Upsilon(nS)$ and weighted mean values for the $\chi_b(nP)$ resonances [16].

- $BR[\Upsilon(1S)\to\mu^+\mu^-] = 2.48$ % ([37])
- $BR[\Upsilon(2S)\to\mu^+\mu^-] = 1.31$ % ([37])
- $BR[\Upsilon(3S)\to\mu^+\mu^-] = 1.81$ % ([37])

Colour-singlet parameters (from [28]):

- $< O_1^{\Upsilon(1S)}(^3S_1) > |_{tot} = 11.1$ GeV^3
- $< O_1^{\Upsilon(2S)}(^3S_1) > |_{tot} = 5.01$ GeV^3
- $< O_1^{\Upsilon(3S)}(^3S_1) > |_{tot} = 3.54$ GeV^3, defined as

$$< O_1^{\Upsilon(nS)}(^3S_1) > |_{tot} \;=\; \sum_{m\geq n}^{3} < O_1^{\Upsilon(mS)}(^3S_1) > Br[\Upsilon(mS)\to\Upsilon(nS)X] \tag{A.4}$$

- $< O_1^{\chi_{b1(1P)}}(^3P_1) >= 6.09$ GeV^5
- $< O_1^{\chi_{b1(2P)}}(^3P_1) >= 7.10$ GeV^5

The radial wave functions at the origin (and their derivatives) used in the generation can be related to the above matrix elements as

$$< O_1^{\Upsilon(nS)}(^3S_1) > = \frac{9}{2\pi}|R_n(0)|^2 \tag{A.5}$$

$$< O_1^{\chi_{bJ(nP)}}(^3P_J) > = \frac{9}{2\pi}(2J+1)|R'_n(0)|^2 \tag{A.6}$$

whose numerical values were obtained from a Buchmüller-Tye potential model tabulated in Ref. [38].

Colour-octet long-distance parameters to be extracted from the fit:

- $< O_8^{\Upsilon(nS)}(^3S_1) > |_{tot}$, defined as

$$\begin{aligned} < O_8^{\Upsilon(nS)}(^3S_1) > |_{tot} \quad &= \sum_{m\geq n}^{3} < O_8^{\Upsilon(mS)}(^3S_1) > Br[\Upsilon(mS)\to\Upsilon(nS)X] \\ &+ \sum_{m\geq n}^{2}\sum_{J=0}^{2} < O_8^{\chi_{bJ}(mP)}(^3S_1) > Br[\chi_{bJ}(mP)\to\Upsilon(nS)X] \end{aligned} \tag{A.7}$$

- $< O_8^{\Upsilon(nS)}(^1S_0) > |_{tot}$, defined as

$$< O_8^{\Upsilon(nS)}(^1S_0) > |_{tot} \quad = \sum_{m\geq n}^{3} < O_8^{\Upsilon(mS)}(^1S_0) > Br[\Upsilon(mS)\to\Upsilon(nS)X] \tag{A.8}$$

- $< O_8^{\Upsilon(nS)}(^3P_0) > |_{tot}$, defined as

$$< O_8^{\Upsilon(nS)}(^3P_0) > |_{tot} \quad = \sum_{m \geq n}^{3} < O_8^{\Upsilon(mS)}(^3P_0) > Br[\Upsilon(mS) \rightarrow \Upsilon(nS)X] \tag{A.9}$$

On the other hand, the differences in shape between the $^1S_0^{(8)}$ and $^3P_J^{(8)}$ contributions were not sufficiently great to justify independent generations for them. In fact, temporarily setting $< O_8^{\Upsilon(1S)}(^3P_0) >= m_b^2 < O_8^{\Upsilon(1S)}(^1S_0) >$ and defining the ratio

$$r(p_T) \;=\; \frac{\sum_{J=0}^{2} \frac{d\sigma}{dp_T}[^3P_J^{(8)}]}{\frac{d\sigma}{dp_T}[^1S_0^{(8)}]} \tag{A.10}$$

it is found $r \simeq 5$ as a mean value over the $[0, 20]$ GeV p_T-range. Actually the above ratio is not steady as a function of the $\Upsilon(1S)$ transverse momentum. Therefore in the generation we split the p_T region into two domains: for $p_T \leq 6$ GeV we set $r = 6$ whereas for $p_T > 6$ GeV we set $r = 4$.

In summary, only the $^1S_0^{(8)}$ channel was generated but rescaled by the factor r to incorporate the $^3P_J^{(8)}$ contribution as we did in [10] for charmonium hadroproduction. Consequently, in analogy to [20] we shall consider only the combination of the colour-octet matrix elements:

$$M_5 \;=\; 5 \times \left(\frac{< O_8^{\Upsilon(1S)}(^1S_0) > |_{tot}}{5} + \frac{< O_8^{\Upsilon(1S)}(^3P_0) > |_{tot}}{m_b^2} \right) \tag{A.11}$$

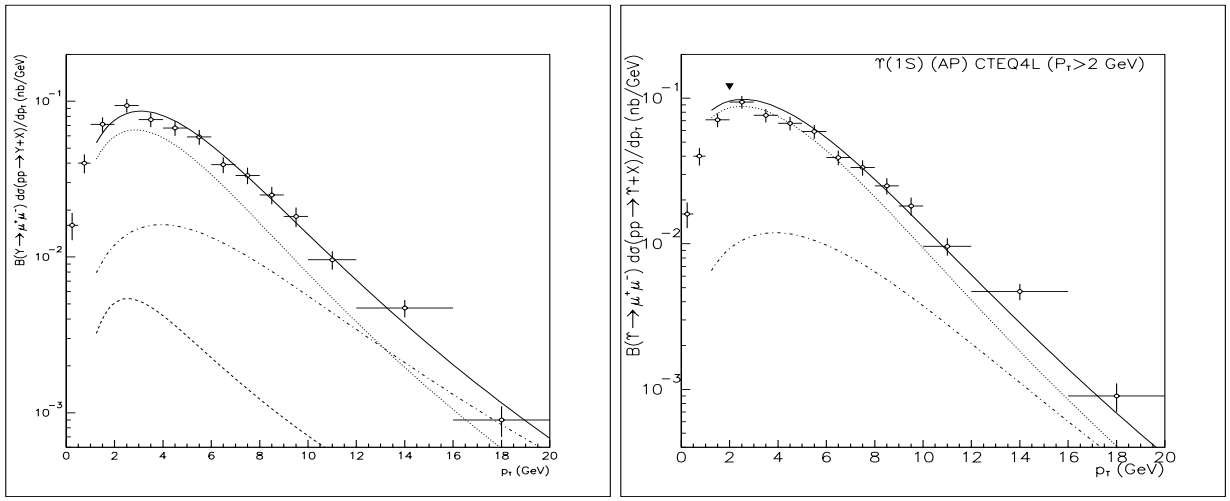

Figure 7: Fits to Tevatron $\Upsilon(1S)$ data using CTEQ2L *(left)* and CTEQ4L *(right)*; dotted line: CSM, dashed line ${}^1S_0 + {}^3P_J$ contribution, dot-dashed line: ${}^3S_1^{(8)}$ contribution, solid line: all contributions.

CTEQ4L versus CTEQ2L

In our previous work [16] on $\Upsilon(1S)$ hadroproduction we employed the (now outdated) CTEQ2L parton distribution function, which however is still often used in current applications of PYTHIA at LHC collaborations. Throughout this paper we have used CTEQ4L but a comparison with the previous analysis is in order. In Figure 7 we present the two fits to the same Tevatron data [26]. Notice that the ${}^1S_0 + {}^3P_J$ contribution has been disregarded in the latter case.

Table 7: Colour-octet matrix elements (in units of 10^{-3} GeV^3) from the best fits to CDF data at the Tevatron on prompt $\Upsilon(1S)$ inclusive production, using either CTEQ2L [15] or CTEQ4L parton distribution functions respectively.

ME:	$< O_8^{\Upsilon(1S)}({}^3S_1) > \vert_{tot}$	$M_5^{\Upsilon(1S)} = 5\times\left(\frac{<O_8^{\Upsilon(1S)}({}^3P_0)>}{m_b^2} + \frac{<O_8^{\Upsilon(1S)}({}^1S_0)>}{5}\right)$
CTEQ2L	139±18	6±5
CTEQ4L	77±17	$\simeq 0$

The CTEQ4L PDF incorporates a BFKL style rise at small x, rather than a flat shape as in CTEQ2L. Therefore it is not surprising that we find smaller values for the colour-octet matrix elements in the former case, as can be seen in Table 7.

B

Altarelli-Parisi evolution

According to the colour-octet model, gluon fragmentation becomes the dominant source of heavy quarkonium direct production at high transverse momentum. On the other hand, Altarelli-Parisi (AP) evolution of the splitting gluon into $(Q\overline{Q})$ produces a depletion of its momentum and has to be properly taken into account. If not so, the resulting long-distance parameter for the ${}^3S_1^{(8)}$ channel would be underestimated from the fit [12].

The key idea is that the AP evolution of the fragmenting gluon is performed from the evolution of the *gluonic partner* of quarkonium in the final-state of the production channel

$$g \ + \ g \rightarrow g^*(\rightarrow (Q\overline{Q})[{}^3S_1^{(8)}]) \ + \ g \tag{B.1}$$

Let us remark that, in fact, g^* is not generated in our code [10]. Final hadronization into a $(Q\overline{Q})$ bound state is taken into account by means of the colour-octet matrix elements multiplying the respective short-distance cross sections [20, 10]. Nevertheless, it is reasonable to assume that, on the average, the virtual g^* should evolve at high p_T similarly to the other final-state gluon - which actually is evolved by the PYTHIA machinery. We used this fact to simulate the (expected) evolution of the (ungenerated) g^* whose momentum was assumed to coincide with that of the resonance (neglecting the effect of emission/absorption of soft gluons by the intermediate coloured state bleeding off colour [11]).

Therefore, event by event we get a correcting factor to be applied to the transverse mass of the $(Q\overline{Q})$ state (for the ${}^3S_1^{(8)}$ channel only):

$$x_{AP} \ = \ \frac{\sqrt{p_T^{*2} + m^2_{(Q\overline{Q})}}}{\sqrt{p_T^2 + m^2_{(Q\overline{Q})}}} \tag{B.2}$$

where p_T (p_T^*) denotes the transverse momentum of the final-state gluon without (with) AP evolution and $m_{(Q\overline{Q})}$ denotes the mass of the resonance. At high p_T,

$$p_T^{AP} \ = \ x_{AP} \times p_T \tag{B.3}$$

where p_T is the transverse momentum of the resonance as generated by PYTHIA (i.e. without AP evolution), whereas for $p_T \leq m_{(Q\overline{Q})}$ the effect becomes much less significant as it should be. Thus the interpolation between low and high p_T is smooth with the right asymptotic limits at both regimes. The above way to implement AP evolution may appear somewhat simple but it remains in the spirit of our whole analysis, i.e. using PYTHIA machinery whenever possible. In fact, it provides an energy depletion of the fragmenting gluon in agreement with previous work on charmonium hadroproduction [20, 12]. In Figure 8 the

x_{AP} factor is plotted as a function of the transverse momentum of the resonance for the Tevatron event generation.

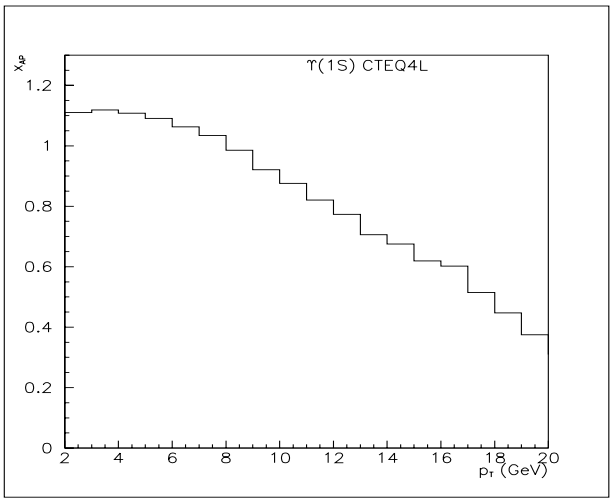

Figure 8: x_{AP} factor as a function of p_T for Tevatron energies obtained from our generation.

Moreover, in order to assess the effect of AP evolution on the fit parameters we show in Table 8 two numerical values for the relevant colour-octet MEs obtained from a best χ^2 fit to Tevatron data [26] using the CTEQ4L PDF: (i) the first row corresponds to a generation *without* AP evolution; (ii) the second one does take it into account. Notice the increase of $< O_8^{\Upsilon(1S)}(^3S_1) > |_{tot}$ in the latter case w.r.t. AP off, but to a lesser extent than for charmonium [12].

Table 8: Colour-octet matrix elements (in units of 10^{-3} GeV^3) from the best fit to CDF data at the Tevatron on prompt $\Upsilon(1S)$ production. The CTEQ4L PDF was used with AP evolution off and on respectively.

ME:	$< O_8^{\Upsilon(1S)}(^3S_1) > \|_{tot}$
AP off	70±15
AP on	77±13

It is worth noting that the effect of the AP evolution on the shape of the differential cross section over the [1,20] GeV p_T-range, though sizeable, is considerably less pronounced for bottomonium than for charmonium [12] because of the larger mass of the former. Nevertheless we can appreciate in Figure 9 that the plot corresponding to AP evolution is noticeably steeper at moderate and high p_T as could be expected. Let us finally remark that, although we can switch on/off AP evolution and initial-state radiation *at will* in the event gener-

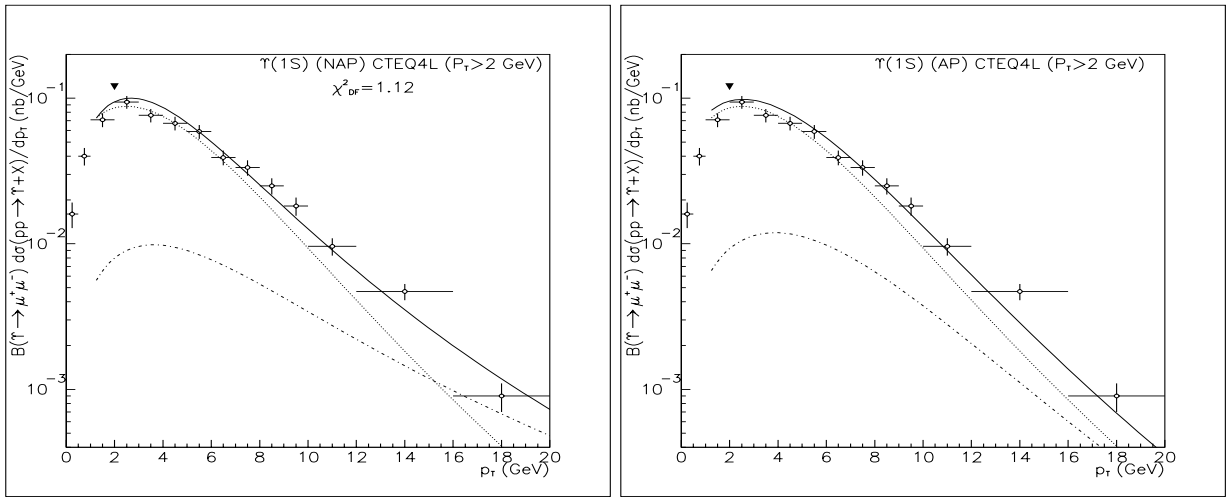

Figure 9: Theoretical curves obtained from a fit using PYTHIA including the colour-octet mechanism for prompt $\Upsilon(1S)$ production against CDF data at the Tevatron *a)* without AP evolution of the fragmenting gluon, *b)* with AP evolution of the fragmenting gluon. The CTEQ4L parton distribution function and $m_b = 4.88$ GeV were employed in the fits; dotted line: CSM, dot-dashed line: ${}^3S_1^{(8)}$ contribution, solid line: all contributions.

ation, both next-to-leading order effects have to be incorporated for a realistic description of the hadronic dynamics of the process.

C

Rapidity cut and azimuthal correlations

In this appendix we show that the (systematic) uncertainty associated to the determination of the Feynman x of the interacting partons in our proposed method, is given by the upper rapidity cut y_0 on the resonance imposed to events, according to the expression:

$$\frac{\Delta x}{x} \;=\; y_0 \tag{C.1}$$

Indeed, assuming a gluon gluon scattering process into two final-state gluons, it is easy to see that any extra (longitudinal) rapidity amount Δy of any final-state parton, should be assigned to anyone of the two colliding partons, as a consequence of conservation of energy-momentum. (In this case the partonic reference frame would not longer coincide with the Lab frame.)

On the other hand, a parton carrying a fraction x of the total hadron momentum has a (longitudinal) rapidity

$$y \;=\; y_{hadron} \;-\; \log\frac{1}{x} \tag{C.2}$$

where y_{hadron} is the rapidity of the hadron in the Lab system.

Differentiating both sides of Eq. (C.2) and setting $\Delta y = y_0$, one gets easily the expression (C.1).

Let us observe that the rapidity cut $|y| < y_0$ binds us to a region of "allowed" transverse momentum, increasing with p_T since $x^2 s \simeq 4p_T^2$, and hence

$$\frac{\Delta p_T}{p_T} \;=\; y_0 \tag{C.3}$$

This means that as the transverse momentum grows, the p_T range compatible with the relative error, predetermined by choosing the value of y_0, grows too. If this value is set very low, the precision on the Feynman x increases but the price to be paid is probably reducing too much the statistics. Conversely, allowing y_0 to be *too large*, leads to larger statistics but spoiling the knowledge of x because of the uncertainty given by (C.1). As a compromise, we chose $y_0 = 0.25$ which, however, could be varied depending on the size of the sample of collected events.

In order to get an idea of the expected impact of the intrinsic k_T on the topology of events, we show in Figure 10 several plots of the transverse momenta of the $\Upsilon(1S)$ resonance versus the recoiling jet. In the absence of any higher order QCD effect, events squeeze along the diagonal. However k_T smearing spreads events over a larger area in the plot, spoiling somehow a naive picture of a back-to-back topology coming from a collinear approximation to leading order; Figure 10.a) corresponds to initial-state radiation activated in the PYTHIA

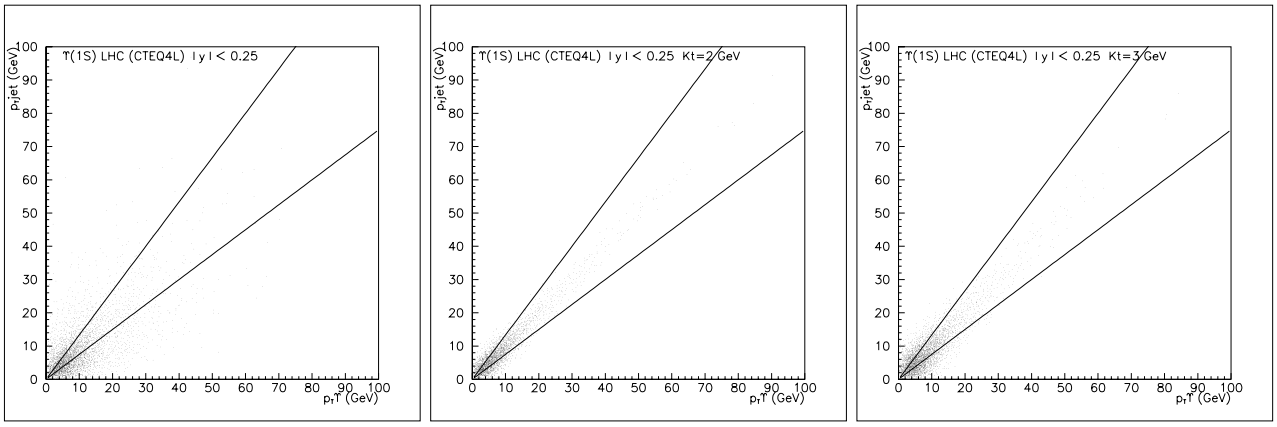

Figure 10: Plots of the jet transverse momentum versus the $\Upsilon(1S)$ resonance transverse momentum at LHC energy (parton/particle level simulation) using, from left to right: *a)* the PYTHIA algorithm to simulate initial-state radiation; using a gaussian smearing function with *b)* $< k_T >= 2$ GeV and *c)* $< k_T >= 3$ GeV. The two straight lines indicate the allowed region according to the p_T uncertainty obtained from Eq. C.3 for $y_0 = 0.25$.

generation following the model developed in [21]. Alternatively, Figures 10.b) and 10.c) show the effect of a gaussian spread of $< k_T >= 2$ GeV and $< k_T >= 3$ GeV, respectively. The region inside the two straight lines corresponds to an uncertainty on p_T given by Eq. (C.3) for a rapidity value $y_0 = 0.25$. Although at small and moderate p_T (say, $p_T \leq 10$ GeV) all plots essentially agree, at higher p_T the former one, corresponding to a full simulation of gluon emission in the initial-state performed by PYTHIA, displays much more events outside the accepted region.

Table 9: Fraction (in %) of events inside the region defined by the two straight lines for different p_T lower cuts (in GeV) applied to the resonance, corresponding to Fig. 10.a), i.e. initial-radiation generated by PYTHIA.

p_T cut-off:	10	20	30	40	50
% "inside"	39 ± 1	38 ± 3	35 ± 5	38 ± 9	38 ± 15

In Table 9 we show the fractions of events inside the allowed region between the two straight lines in the plot 10.a) (initial-state radiation on). We observe that about 40% of all events are "accepted", remaining practically constant above $p_T = 10$ GeV. Finally we conclude that such reduction factor (of the order of 40%) does not represent in itself a dramatic loss of statistics regarding our proposed method to probe the gluon density in protons. On the other hand, for the gaussian smearing, the situation is even much more optimistic.

In Figures 11 we show the azimuthal $\Delta\phi$ angle between the muon pair direction

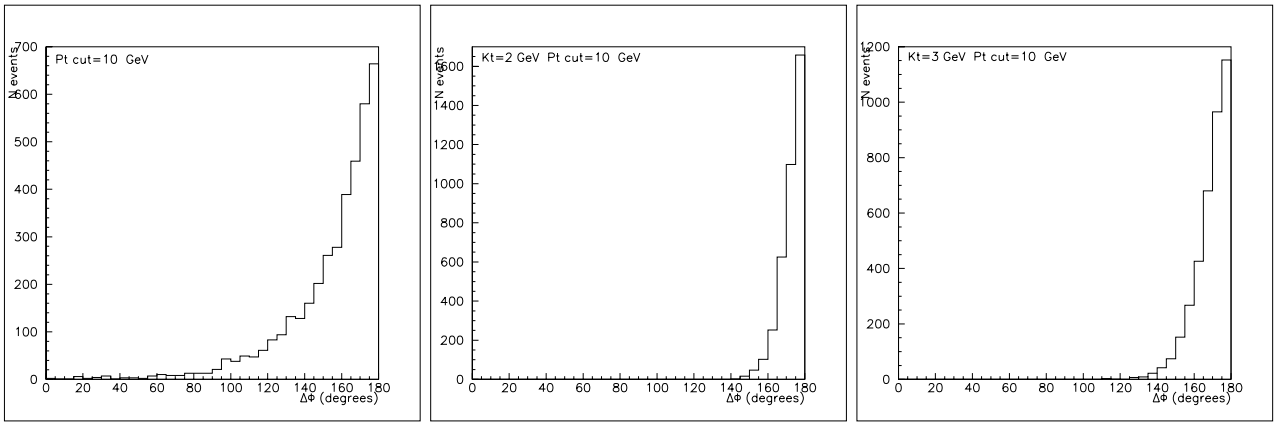

Figure 11: Azimuthal angle between the recoiling jet direction (defined by the parent gluon momentum) and the dimuon direction from $\Upsilon(1S)$ decays in the transverse plane, from left to right: *a)*: Initial-state radiation activated in PYTHIA; *b)* Using gaussian smearing with $< k_T >= 2$ GeV; *c)* The same with $< k_T >= 3$ GeV. All plotted events were selected with $\Upsilon(1S)$ transverse momentum greater than 10 GeV.

(defining the direction of the fragmenting gluon into bottomonium) and the recoiling jet generated by the final-state gluon, for different values of the effective k_T, in correspondence with Figures 10. In Fig. 11.a) we used the PYTHIA algorithm for initial-state radiation, whereas in Figures 11.b) and 11.c) we used a smearing gaussian with $< k_T >= 2$ GeV and $< k_T >= 3$ GeV, respectively. As expected, again we realize the sizeable effect of the effective k_T effect on the distribution, especially in the former case. Nevertheless, most events should display a clear enough back-to-back signature as regards the $\Delta\phi$ variable (in addition to the p_T balance), as indicated by the peak at 180 degrees in all plots of Figure 11.